Water-Soluble Polymers. LXXXIII. Correlation of Experimentally Determined Drag Reduction Efficiency and Extensional Viscosity of High Molecular Weight Polymers in Dilute Aqueous Solution

MARTIN E. COWAN, CHAD GARNER, ROGER D. HESTER, CHARLES L. MCCORMICK

Department of Polymer Science, University of Southern Mississippi, Hattiesburg, Mississippi 39406

Received 27 October 2000; accepted 27 December 2000

ABSTRACT: The extensional viscosity for aqueous solutions of high molecular weight poly(acrylamide) copolymers and poly(ethylene oxide) homopolymers was measured using a laboratory-designed screen extensional rheometer. A Bingham model was developed to estimate the average local polymer coil extensional viscosity (η_{coil}). A strong correlation was found between the measured η_{coil} values and the polymer extensional viscosity predicted by a bead-spring model. The dilute aqueous solution drag reduction was measured with a rotating disk instrument under conditions minimizing the effects of shear degradation. Extensional viscosity and drag reduction measurements were performed in deionized water and in 0.514*M* sodium chloride. The relative drag reduction efficiency values (Δ) in both solvents were found to strongly correlate with measured η_{coil} values. This is the first report of the accurate prediction of drag reduction behavior for a wide range of polymer types in various solvents from the independently measured molecular parameters η_{coil} and $[\eta]C$. The often-used relative drag reduction efficiency expressed as the product of $[\eta]C$ and Δ can now be replaced by the absolute drag reduction efficiency $[\eta]C\eta_{coil}$. © 2001 John Wiley & Sons, Inc. J Appl Polym Sci 82: 1222–1231, 2001

Key words: water-soluble polymers; drag reduction efficiency; extensional viscosity

INTRODUCTION

It has been known for years that certain additives reduce the frictional energy of turbulent flow. This phenomenon, termed drag reduction (DR),[1] was first reported by Toms in 1948 for dilute solutions of high molecular weight polymers.[2] Under turbulent flow conditions, regions of chaotic flow (turbulence) develop that are responsible for loss of flow efficiency.[3] Drag-reducing additives diminish turbulence, resulting in increased flow efficiency.[4–8] In spite of many attempts to explain the DR mechanism(s),[9–11] a universally accepted predictive model is still lacking. Over the years, polymer extensional viscosity has attracted considerable attention as a possible mechanism for turbulence suppression in DR.[5,12,13]

Schummer and Thielen[14] observed an underestimation of the Reynolds shear stresses in turbulent pipe flow for drag-reducing fluids that was attributed to polymer elasticity. Giesekus[15] was the first to suggest that the Reynolds stress deficit was due to an increased local polymer viscosity. Bewersdorff and Berman[16] related the concept of

Correspondence to: C. L. McCormick.

Contract grant sponsors: Gillette Research Institute; Department of Energy.

Journal of Applied Polymer Science, Vol. 82, 1222–1231 (2001)

increased viscosity to the phenomenological aspects of DR, which are onset and saturated DR. The increased local viscosity was proposed to arise from polymer extensional viscosity,[16] known to be orders of magnitude greater than shear viscosity.[17]

Extensional viscosity in dilute polymer solutions arises from resistance of individual polymer molecules to elongation.[17] The technique most used to measure the extensional viscosity of isolated polymer chains is flow through converging and diverging channels of porous media that serve to establish oscillatory extension–compression flow fields.[18] The subjection of dilute solutions of high molecular weight polymers to the oscillatory flow fields results in enormous increases in flow resistance as compared with a solvent.[19–21]

If extensional viscosity is the primary DR mechanism, theoretical models predicting extensional viscosity should correlate somewhat to DR. Hassager[22] used a Zimm bead-spring model[23] to examine the uncoiling of a polymer chain in pure constant strain and developed eqs. (1a) and (1b) (when solved for η_{el})

$$\frac{\eta_{el} - 3\eta_0}{3\eta_0} = 2C[\eta]N\left(1 - \frac{1}{2\gamma\tau_p} + \cdots\right) \quad \text{for } \gamma\tau_p > 0.5 \quad (1a)$$

$$\eta_{el} = 3\eta_0[1 + 2C[\eta]N + \cdots] \quad (1b)$$

in which η_{el} is the local polymer elongational viscosity, η_0 is the solvent shear viscosity, C is the polymer concentration, $[\eta]$ is the polymer intrinsic viscosity, N is the degree of polymerization, γ is the elongation rate, and τ_p is the polymer relaxation time. Safieddine[24] and Mumick et al.[25] examined a wide range of polymer types under various solvent conditions and showed a strong correlation between DR behavior and the product of C, $[\eta]$, and N [from eq. (1b)] under constant flow conditions. These findings further support the idea that polymer extensional viscosity is involved in the DR process. However, to date, no studies have been performed in which simultaneous measurements of the extensional viscosity and DR behavior have been examined.[11]

The DR behavior of polymers with widely varying compositions, structures, and molecular weights has been extensively studied in our research group.[11,25–29] The DR data can be directly compared when normalized for a polymer volume fraction ($[\eta]C$), thus offering a facile means for comparing DR efficiency (DRE). The most efficient drag-reducing polymers have the greatest value of percentage of DR (%DR)/$[\eta]C$ at a given polymer volume fraction. The DRE is an indication of the effectiveness with which polymer coils in solution interact with and suppress microvortices present in turbulent flow. The DRE relative to poly(ethylene oxide) (PEO) was quantified by employing a shift factor Δ to yield a universal (volume fraction normalized) DR curve. Values of Δ greater than one indicate more efficient DR while Δ values less than one indicate less efficient DR relative to PEO.

To examine the role of extensional viscosity in DR, a screen extensional rheometer (SER) was designed by our research group that employs fine nylon mesh screens placed in series to create an oscillatory flow field similar to that found in a flow through porous media. A Bingham model, consisting of a strain lock and dashpot in parallel, was utilized to develop eq. (2) for determining the extensional properties of polymer solutions from pressure profiles obtained with the SER.[30]

$$\Delta P_{solution} - \Delta P_0 = \frac{k_s \eta_{coil}}{\beta} Q \quad (2)$$

where $\Delta P_{solution}$ and ΔP_0 are the pressure drops across the screen set for the polymer solution and solvent, respectively; k_s is a slippage factor, assumed to be one for our calculations; η_{coil} is the average local polymer coil extensional viscosity; Q is the volumetric flow rate; and β is a collection of constants defined in eq. (3).

$$\beta = \frac{\pi D^2 d_{wire} f^2}{64 n \varphi 4 \eta_{intr}(1 - f)^2} \quad (3)$$

where D is the screen diameter, d_{wire} is the diameter of the nylon filaments that make up the screen, f is the fractional free projected area, n is the number of screens, ϕ is the porosity, and η_{intr} is the zero shear intrinsic viscosity of the polymer solution. All of the variables in eqs. (2) and (3) are either known or can be measured, allowing determination of η_{coil}. The value of η_{coil} is an estimate of the increased average local viscosity of individual polymer coils undergoing extension. Increased local viscosity upon deformation provides an energy conversion mechanism whereby fluid kinetic energy is converted to heat, possibly pro-

Table I Polymer Composition (mol %) and Comonomer Chemical Structures

Polymer	AM	DAAM	NaAMB	AMPTAC
PAAm	100			
DAAM 33	67	33		
NaAMB 15	85		15	
ATABAM 3.3-3.7	93		3.3	3.7

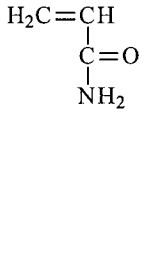

AM

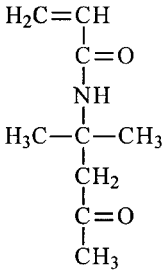

DAAM

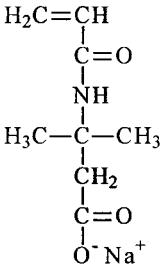

NaAMB

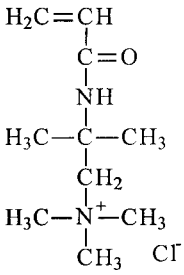

AMPTAC

viding the energy conversion mechanism responsible for the reduction of turbulence in DR.

The purpose of our continuing DR research is to further explore the relationship between polymer extensional viscosity and DRE using structurally tailored water-soluble copolymers. A comparison of DR behavior for anionic, nonionic, and zwitterionic water-soluble polymers with measured and theoretically predicted extensional viscosity values was undertaken to provide further insight into the role of extensional viscosity in DR.

EXPERIMENTAL

Monomer and Polymer Synthesis

Acrylamide (AAm), diacetone acrylamide (DAAM), and potassium persulfate (K_2SO_8) were purchased from Aldrich. The AAm and DAAM were recrystallized twice from acetone while K_2SO_8 was recrystallized twice from deionized water prior to use. Union Carbide supplied the PEO samples WSR 1105, WSR N60K, and WSR 301 with reported viscosity-average molecular weights of 0.9×10^6, 2×10^6, and 4×10^6 g/mol, respectively. These were used as received after vacuum drying.

The polymers utilized in this study included homopoly(acrylamide) (PAAm), copolymers of AAm with DAAM, sodium 3-acrylamido-3-methylbutanoate (NaAMB), and a terpolymer of AAm with NaAMB and 2-(acrylamido)-2-methylpropanetrimethylammonium chloride (AMPTAC) (Table I). The NaAMB was synthesized by a Ritter reaction of 3,3-dimethyl acrylic acid with acrylonitrile as reported by Hoke and Robbins[31] and modified by Blackmon.[32] The AMPTAC was synthesized as previously reported.[33]

All acrylamido polymers were synthesized via free-radical solution polymerization in deionized water[32] with K_2SO_8 as the initiator. The polymerizations were halted by precipitation in acetone and the polymer product was purified by dialyzing against deionized water using Spectra/Por 4 dialysis bags with a molecular weight cutoff of 12,000–14,000 Da. After dialysis the polymer solutions were lyophilized to yield white, cottonlike solids.

Polymer solutions were prepared using deionized water (18.2 MΩ resistivity) and allowed to age for at least 1 month with 0.01% (w/w) sodium azide as a biocide.

Characterization

^{13}C-NMR Spectroscopy

^{13}C-NMR spectra were obtained using a Bruker AC 300 spectrometer for concentrated polymer solutions in D_2O with DSS as a reference. Integration of the carbonyl peaks of the various comonomers allowed the determination of copolymer compositions as previously outlined.[34]

Viscometry

The low shear intrinsic viscosity [η] measurements were performed with a Contraves LS30 low shear viscometer at a shear rate of 5.9/s. The intrinsic viscosity values for each polymer solution were determined by extrapolating reduced[35] and inherent viscosity[36] values to zero concentration.

Multiangle Laser Light Scattering

The refractive index increments were determined using a Chromatix KMX-16 laser differential refractometer. The polymer solutions were clarified using a 1-mm pore size filter. The polymer concentration was measured before and after filtration for the PAAm by UV spectroscopy to confirm that no polymer was lost during filtering. Classical light scattering measurements were performed at 25°C using a Brookhaven Instruments BI-200SM automatic goniometer interfaced with a personal computer. Excess scattered intensity measurements were obtained at multiple angles between 30 and 150°. Zimm plots were generated using software provided by the manufacturer.

DR Measurements

The DR measurements were performed using a rotating disk instrument designed in our laboratories. The instrument consists of an 18.5-L cylindrical tank (30.5-cm o.d., 0.953-cm wall thickness) with a removable polycarbonate cover. A 9-cm radius stainless steel disk and spindle assembly driven by a Maxon 80-W dc motor provides the external rotational flow field. The spindle assembly rests in a bushing at the bottom of the sample vessel to stabilize the disk during rotation. An HP HEDS-6310 optical tachometer and a Vibrac TQ-100 torque transducer constantly measure the instrument performance while a computer utilizing National Instrument's LabView® software controls the rotational speed of the disk and records rotational speed and torque in real time.

Stock solutions were prepared and allowed to age for at least 1 month using 0.01 wt % sodium azide as a biocide. For each experiment the proper amount of stock solution was diluted to the desired concentration. The %DR is defined as the percentage of torque difference required to rotate the disk at a given revolutions per minute for a solvent and polymer solution as shown in eq. (4):

$$\% \text{ DR} = \frac{T_0 - T_{\text{polymer}}}{T_0} \times 100 \qquad (4)$$

where T_0 and T_{polymer} are the torque values for the solvent and polymer solution, respectively. To minimize the effects of shear degradation, only values for T_{polymer} measured near time zero were utilized in all calculations. The DR data were found to be reproducible to within $\pm 2\%$.

Extensional Viscosity Measurements

Extensional viscosity measurements were performed using the SER developed in our laboratories. An ISCO 500D syringe pump provided controlled flow and the pressure was measured before and after the screen set by two pressure transducers. The data were recorded in real time with a PC using LabView data acquisition software.

RESULTS AND DISCUSSION

Copolymer Structural Data

The acrylamido polymer compositions and monomer structures utilized in this study are listed in Table I.[26,32,37,38] The DAAM copolymer has 33 mol % DAAM and 67 mol % AAm and the NaAMB copolymer has 15 mol % NaAMB. The terpolymer consists of 3.3 mol % NaAMB and 3.7 mol % AMPTAC.

The intrinsic viscosity values determined in 0.514*M* NaCl and dionized water (except for NAMB copolymers) are shown in Table II. Classical light scattering data for all of the polymers (including the commercially supplied PEO samples) are also reported in Table II. The molecular weights for the PEO samples ranged from (0.55 to 4.3) $\times$ 10^6 g/mol while the acrylamido polymers ranged from (0.65 to 1.89) $\times$ 10^6 g/mol.

Extensional Viscosity Measurements

The extensional viscosity of macromolecules in turbulent flow was suggested as a possible mechanism responsible for polymeric DR in dilute solution.[5,12,13,39] The extensional viscosity was measured for dilute solutions ($[\eta]C = 0.1$) of each of the polymers in this study utilizing our SER.

An example of the pressure profiles attained for polymer solutions of PEO in deionized water flowing through a set of 30 screens is shown in Figure 1. The pressure profiles for all polymers examined with the SER had several common features. At low flow rates the measured pressure across the screens was the same for the solvent

Table II Molecular Weight and Dilute Solution Viscosity Characterization of Drag-Reducing Polymers

Polymer	dn/dc	M_W ($\times 10^{-6}$ g/mol)	$[\eta]^a$ (dL/g)	$[\eta]^b$ (dL/g)
PAAm	0.176	1.89	15.2	16.3
DAAM 35	0.173	0.69	8.4	6.4
NaAMB 25	0.158	1.43	NA	13.5
ATABAM 55	0.175	0.65	11.6	12.5
WSR 301	0.158	4.3	18.6	14.3
WSR N60K	0.144	2.0	10.1	8.3
WSR 1105	0.147	0.55	5.5	5.4

dn/dc, the refractive index increment; M_W, the weight-average molecular weight determined by MALLS; $[\eta]$, the polymer intrinsic viscosity.
[a] In deionized water.
[b] In 0.514*M* aqueous NaCl solution.

and polymer solution. At some critical flow rate (Q_{yield}) the pressure for the polymer solution began to increase considerably relative to the solvent. The Q_{yield} was strongly dependent on the polymer molecular weight with values of 100, 36, and 12 mL/min for PEO samples with molecular weights of 0.55×10^6, 2.0×10^6, and 4.3×10^6 g/mol, respectively. The Q_{yield} is thought to be the flow rate at which the polymer coils begin to extend. According to Hassager,[22] the elongation rate required to extend a macromolecule is inversely proportional to the square of the molecular weight. A plot of $1/Q_{yield}$ versus the square of the molecular weight is illustrated in Figure 2. A correlation coefficient of nearly one strongly suggested that the Q_{yield} was the flow rate corresponding with the onset of polymer elongation.

At flow rates above Q_{yield}, the slope of the pressure versus the flow rate increased with increasing molecular weight (Fig. 1) and was directly related to the local viscosity of the polymer coils (η_{coil}) by eq. (2). The η_{coil} values for each of the polymers examined in this study in deionized water and 0.514*M* NaCl solution are listed in Table III. As with the intrinsic viscosity values, only small differences in η_{coil} were observed with changing ionic strength. The polymer samples with the greatest extensional viscosity were WSR 301, WSR N60K, and PAAm with η_{coil} values in deionized water of 3.27, 1.72, and 1.34 P, respec-

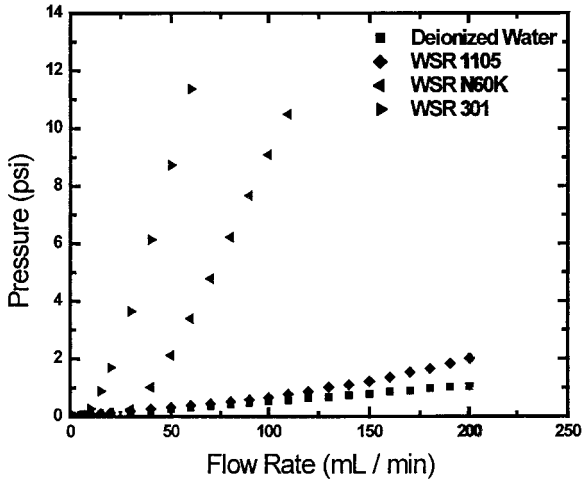

Figure 1 The pressure response for PEO samples of different molecular weights in deionized water versus the flow rate as measured with the screen extensional rheometer. The molecular weights of the PEO samples were 0.55×10^6 g/mol for WSR 1105, 2.0×10^6 g/mol for WSR N60K, and 4.3×10^6 g/mol for WSR 301.

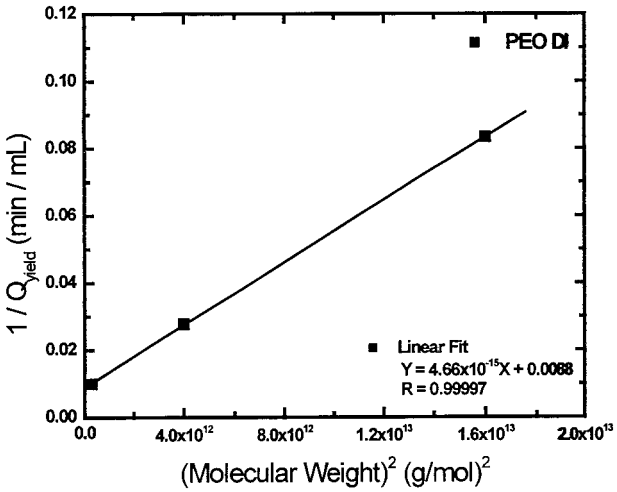

Figure 2 The inverse Q_{yield} values versus the square of the polymer molecular weight for PEO samples in deionized water as measured with the screen extensional rheometer.

Table III Extensional Viscosity in Deionized Water and 0.514*M* Aqueous NaCl Solution

Polymer	η_{coil} (P) Deionized Water	η_{coil} (P) 0.514*M* NaCl
PAAm	1.34	0.96
DAAM 33	0.017	0.025
NaAMB 15	NA	0.009
ATABAM 3.3, 3.7	0.41	0.44
WSR 1105	0.11	0.04
WSR N60K	1.72	1.89
WSR 301	3.27	3.58

η_{coil}, the average coil viscosity as measured with the screen extensional rheometer.

tively, and η_{coil} values in 0.514*M* NaCl solution of 3.58, 1.89, and 0.96 P, respectively. The DAAM 33, WSR 1105, and ATABAM 3.3-3.7 samples yielded much lower extensional viscosity with η_{coil} values in deionized water of 0.41, 0.11, and 0.017 P, respectively, and η_{coil} values in 0.514*M* NaCl solution of 0.44, 0.04, and 0.025 P, respectively. The η_{coil} value for the NaAMB 25 sample in 0.514*M* NaCl was measured as 0.009 P. The η_{coil} value was not determined in deionized water because of the inability to accurately measure the $[\eta]$ value.

Correlation between η_{coil} and Predicted Polymer Extensional Viscosity

Hassager[22] used a Zimm bead-spring model to develop a relationship predicting reduced polymer extensional viscosity to be proportional to the product of the polymer concentration, intrinsic viscosity, and degree of polymerization ($C[\eta]N$). A direct correlation is seen in Figure 3 when the η_{coil} values determined with the SER are plotted versus $3\eta_0(1 + 2C[\eta]N)$ from eq. (1b). The origin of the difference observed between the theoretical and measured values is not known at this time. The direct correlation validated the use of the SER and Bingham model to measure the extensional viscosity of extremely dilute polymer solutions.

Volume Fraction Normalization of Acrylamido Polymers

When normalized for the volume fraction, the DR data for polymers of widely varying structures

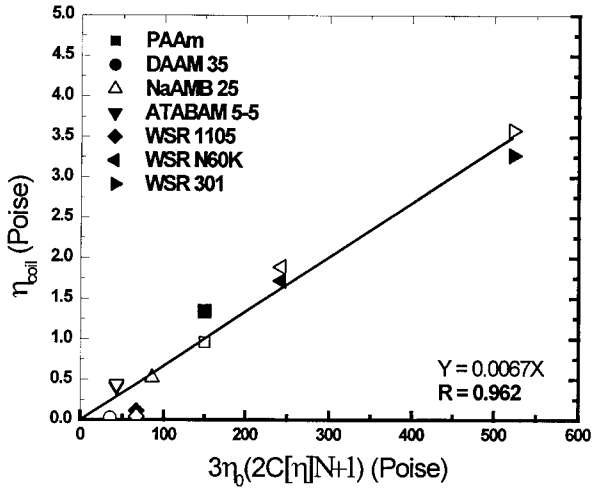

Figure 3 The coil viscosity versus eq. (1b) in deionized water (solid symbols) and 0.514*M* aqueous NaCl solution (open symbols) at 1000 rpm.

and molecular weights were shown to conform to a universal DR curve[26] that allowed a facile comparison of the DRE. A correlation with the volume fraction is attractive to polymer scientists because fundamental contributions of the polymer molecular weight and polymer–solvent interactions are considered.

The DR values normalized for the volume fraction for all the polymers examined in this study are shown in Figure 4 (deionized water) and Figure 5 (0.514*M* NaCl). The DRE for the polymer samples in deionized can be ranked as follows: WSR 301 > WSR N60K > PAAm > ATABAM 3.3-3.7 > DAAM 33 > WSR 1105. In 0.514*M* NaCl

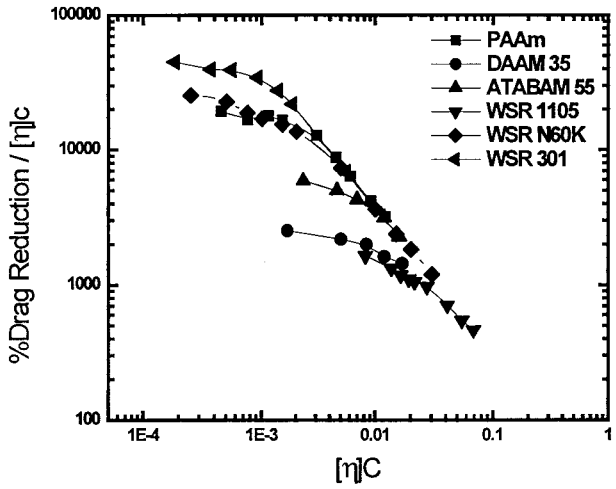

Figure 4 The volume fraction normalization of the drag reduction data in deionized water at 1000 rpm.

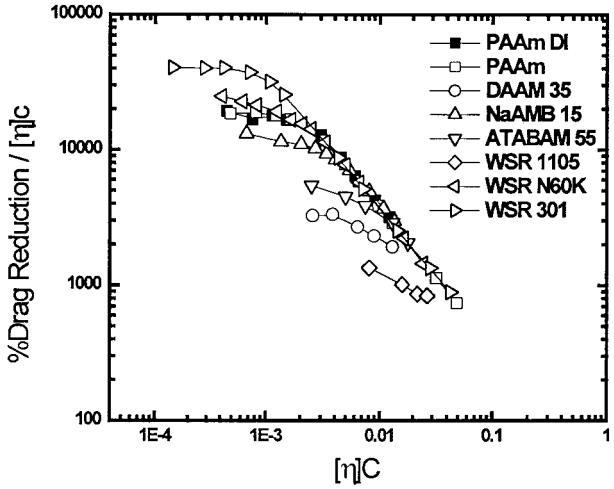

Figure 5 The volume fraction normalization of the DR data in 0.514*M* NaCl at 1000 rpm. The normalized drag reduction data for PAAm in deionized water (chosen as the reference polymer in this study) is included for comparison.

the ranking stays the same with NaAMB 15 falling between the PAAm and ATABAM 3.3-3.7 samples. Shifting each data set by a factor Δ to superimpose the PAAm curve (deionized water) resulted in the curves shown in Figures 6 and 7 with the individual Δ values in both solvents listed in Table IV. PAAm was chosen as the benchmark polymer because it is the base structure for all of the modified poly(acrylamido) polymers and because its DR behavior changes little with changing ionic strength.

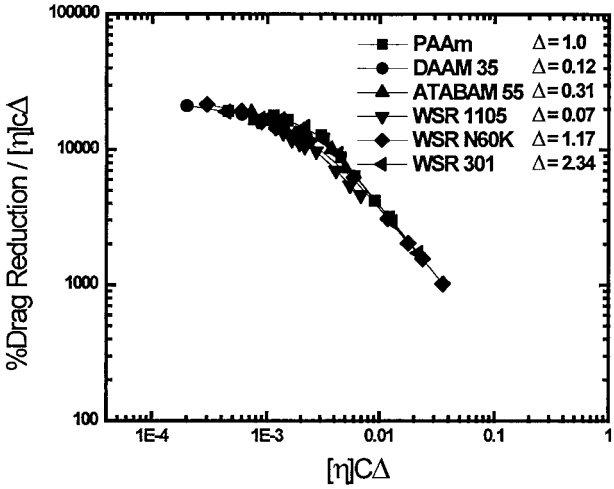

Figure 6 The normalized drag reduction data of all polymers in deionized water shifted using Δ to quantify the drag reduction efficiency relative to PAAm in deionized water.

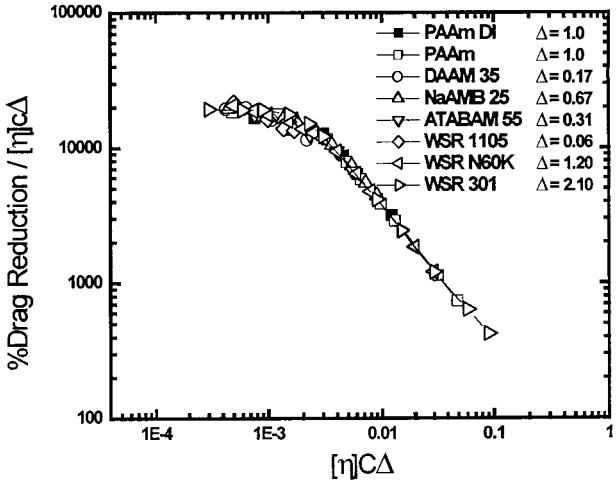

Figure 7 The normalized drag reduction data of all polymers in 0.514*M* aqueous NaCl solution shifted using Δ to quantify the drag reduction efficiency relative to PAAm in deionized water.

Extensional Viscosity Parameter

Figure 8 plots the DR data in deionized water and 0.514*M* NaCl versus $C[\eta]N$ from Hassager's theory of extensional viscosity . In accordance with earlier findings,[24,25] a strong correlation was found between %DR values and the molecular parameters predicted to be important in extensional viscosity for all of the polymers in this study under both solvent conditions (with the exception WSR 1105). The reason for the poor fit of the WSR 1105 data is unclear.

Similar to the Δ, the $C[\eta]N$ parameter normalized the DR data for most of the polymer samples examined in this study. Because $C[\eta]N$ is directly related to η_{coil} (Fig. 3), the relationship between

Table IV Empirical Drag Reduction Efficiency Factor (Δ) in Deionized Water and 0.514*M* Aqueous NaCl Solution

	Δ	
Polymer	Deionized Water	0.514*M* NaCl
PAAm	1.00	1.00
DAAM 35	0.12	0.17
NaAMB 25	NA	0.67
ATABAM 55	0.31	0.31
WSR 1105	0.07	0.06
WSR N60K	1.17	1.20
WSR 301	2.34	2.10

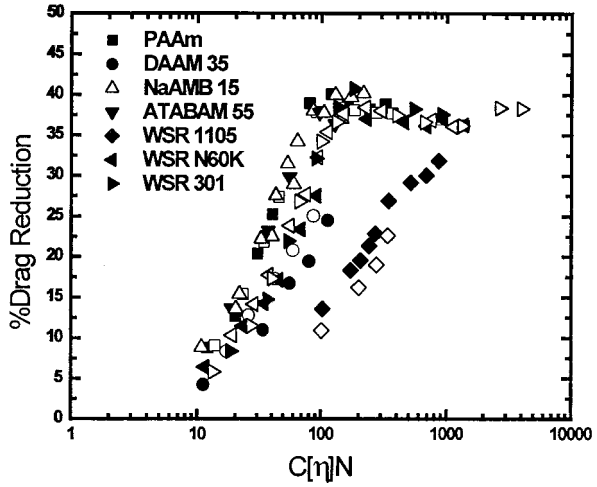

Figure 8 The percentage of drag reduction versus the $C[\eta]N$ in deionized water (closed symbols) and 0.514*M* aqueous NaCl solution (open symbols) at 1000 rpm.

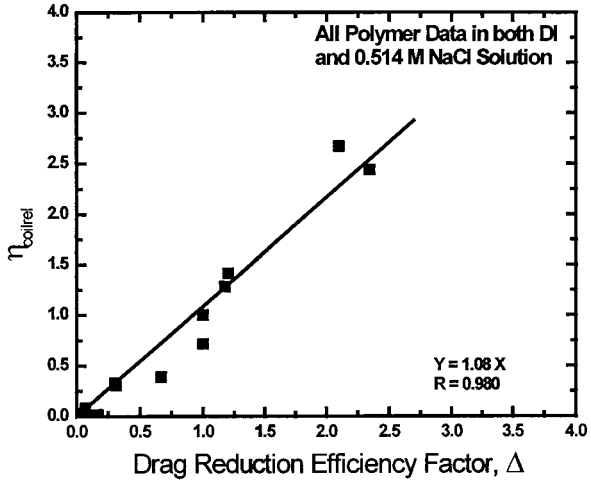

Figure 10 The values for coil normalized relative viscosity values (coilrel) relative to PAAm in deionized water for all polymers examined in this study in deionized water and 0.514*M* NaCl solution versus the empirical drag reduction efficiency factor (Δ).

the extensional viscosity and DRE (represented quantitatively by Δ) can be shown by plotting η_{coil} values versus Δ values (Fig. 9) for each polymer in deionized water and 0.514*M* NaCl. A strong correlation was observed between the η_{coil} values and the Δ parameter for each polymer in both solvents.

For these drag-reducing systems the value for Δ was determined relative to PAAm in deionized water; however, the η_{coil} values were absolute for each polymer. Normalization of the η_{coil} values relative to PAAm in deionized water provided a more consistent comparison between Δ and η_{coil} values. Dividing each η_{coil} value by the η_{coil} value for PAAm in deionized water yielded a value relative to PAAm ($\eta_{coilrel}$). As with Δ, the value for $\eta_{coilrel}$ for PAAm was equal to one. Figure 10 is a plot of $\eta_{coilrel}$ values versus Δ values for each polymer sample in deionized water and 0.514*M* NaCl. A slope of 1.08, an intercept of zero, and a correlation coefficient of 0.980 strongly suggested that Δ and $\eta_{coilrel}$ were equivalent. This was an important finding considering that the two parameters were derived from data acquired by different instruments measuring different flow phenomena.

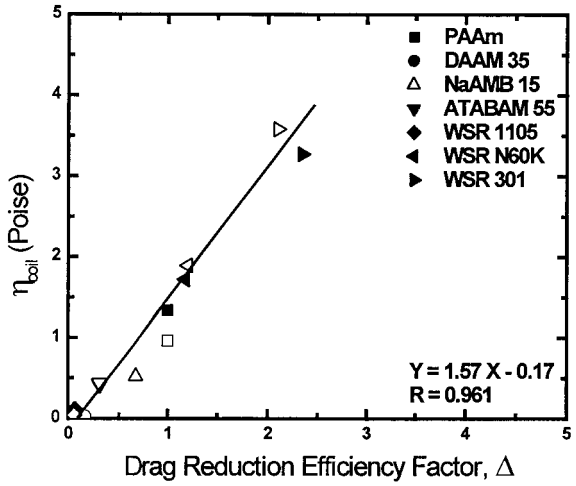

Figure 9 The coil viscosity values versus the empirical drag reduction efficiency factor (Δ) in deionized water (closed symbols) and 0.514*M* aqueous NaCl solution (open symbols).

The Δ values represent DRE on a polymer volume fraction basis. Given the relationship between Δ and η_{coil} values, DR should be dependent on the local polymer η_{coil}, as well as the $[\eta]C$. Figure 11 plots DR data measured with the rotating disk instrument versus the product of η_{coil} (measured with the SER) and polymer volume fraction. All of the DR data fell onto one universal curve with the exception of that from DAAM 33 (a much more efficient drag-reducing polymer than expected from the extensional viscosity measurement). The surface active properties and tendency to form multimolecular aggregates in solution may have been responsible for the high DRE values.[28] The data from the other polymer samples in Figure 11 suggested that the DR behavior can be accurately predicted for a given polymer volume fraction of known local extensional viscosity.

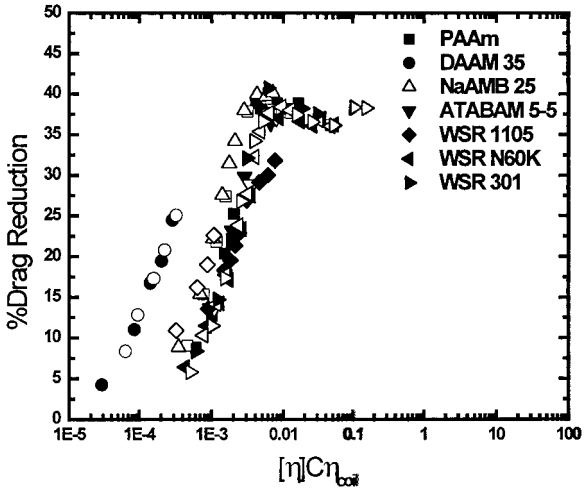

Figure 11 The drag reduction data for all of the polymers examined in this study in deionized water (closed symbols) and 0.514*M* NaCl solution (open symbols) measured at 1000 rpm versus the product of the polymer volume fraction $[\eta]C$ and the local polymer viscosity measured with the SER ($[\eta]C\eta_{coil}$).

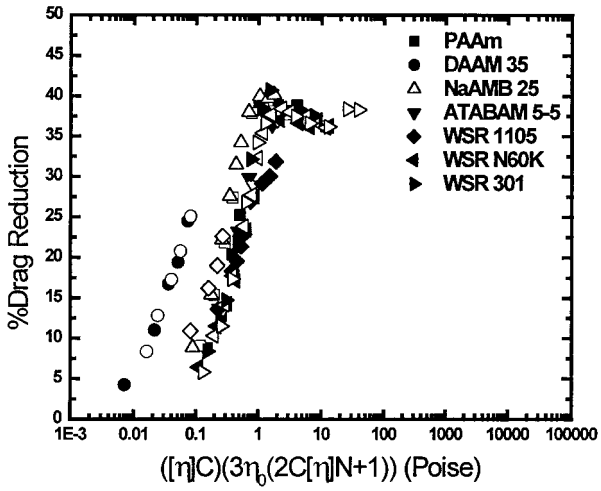

Figure 12 The drag reduction data for all of the polymers examined in this study in deionized water (closed symbols) and 0.514*M* NaCl solution (open symbols) measured at 1000 rpm versus the product of the polymer volume fraction $[\eta]C$ and variables from eq. (1).

For the first time, we report the accurate prediction of DR behavior for a wide range of polymer types in various solvents from the independently measured molecular parameters, η_{coil}, and $[\eta]C$. The relative DR normalization achieved by the use of $[\eta]C\Delta$ can now be replaced by an absolute DRE value $[\eta]C\eta_{coil}$.

Given the strong correlation between the molecular parameters from eq. (1b) and the η_{coil} values (Fig. 3) and between the η_{coil} values and Δ values, normalization of the DR behavior should be possible using the molecular parameters from eq. (1b). Figure 12 plots the DR data versus the product of the polymer volume fraction ($[\eta]C$) and $3\eta_0(1+ 2C[\eta]N)$ (from Fig. 3) to generate a set of curves similar to those in Figure 11. The universal curves in Figures 11 and 12 represent the turbulence reduction expected for polymer solutions of known concentration, intrinsic viscosity, and extensional viscosity behavior. Figures 11 and 12 represent the quantified effect that well-characterized polymer samples have on the turbulence profile of this flow system. These universal curves should be unique to this rotating disk instrument operating at a selected rotational disk speed. Instrument or disk speed changes result in different turbulence distributions with the accompanying differences in turbulence reduction profiles. The DR data obtained at multiple revolutions per minute values with well-characterized dilute polymer solutions allowed the turbulence profile of our rotating disk to be indirectly observed (Fig. 13).

CONCLUSIONS

Several acrylamido polymers were synthesized. Along with commercially supplied PEO samples, they were characterized to determine the molec-

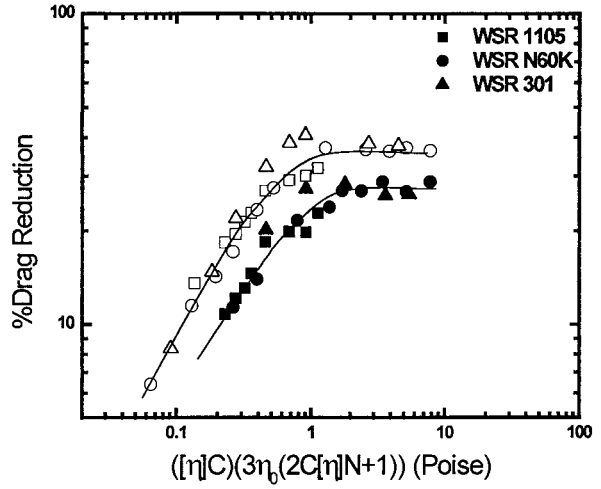

Figure 13 The drag reduction data for aqueous solutions of PEO measured at 800 (closed symbols) and 1000 rpm (open symbols) versus the product of the polymer volume fraction $[\eta]C$ and variables from eq. (1).

ular composition, molecular weight, and dilute solution properties. A SER developed in our laboratories was used to measure the extensional viscosity behavior of the various polymer samples in deionized water and 0.514*M* NaCl. A Bingham model was developed allowing the estimation of a unique extensional viscosity parameter η_{coil} for each polymer sample. The η_{coil} values correlated well with values predicted from theory. The DR behavior was measured for each polymer system in deionized water and 0.514*M* NaCl solution and quantified relative to PAAm using an empirical shift factor Δ. A strong correlation was observed between the DRE (represented by Δ) of the polymer samples and the extensional viscosity behavior (represented by η_{coil}). The DR data conformed to a universal curve when plotted versus the $[\eta]C\eta_{coil}$ and $([\eta]C)\{3\eta_0(1 + 2C[\eta]N)\}$. The universal curves represented the turbulence reduction profile for the fluid system at a given flow condition. Determination of universal curves under multiple flow conditions allowed the DR behavior to be predicted for well-characterized polymer samples. For the first time to our knowledge, well-characterized polymer solutions can be used to characterize the turbulence profile of a flow system and serve as standards for predicting DR behavior of other polymer samples.

The financial support from the Gillette Research Institute and the Department of Energy is gratefully acknowledged. Jim Slemp of Radical Systems, Huntsville, AL, and Steve Selph of the University of Southern Mississippi are greatly appreciated for assisting with the data acquisition and control system.

REFERENCES

1. Savins, J. G. Soc Petroleum Eng J 1964, 4, 203.
2. Toms, B. A. In First International Congress on Rheology, 1948; Amsterdam: North Holland, 1948.
3. Davies, J. T. Turbulence Phenomena; Academic: New York, 1972.
4. Donohue, G. L.; Tiederman, W. G.; Reischman, M. M. J Fluid Mech 1972, 56, 559.
5. Tulin, M. P. In 6th Symposium on Naval Hydrodynamics, 1966; ONR: Washington, DC, 1966.
6. Pfenninger, W. Northrop Corp. Norair Division: 1967.
7. Peterlin, A. Nature 1970, 227, 598.
8. Latto, B.; Shen, C. H. Can J Chem Eng 1970, 48, 34.
9. Shenoy, A. V. Colloid Polym Sci 1984, 262, 455.
10. Kulicke, W.-M.; Kotter, M.; Grager, H. Advances in Polymer Science; Springer–Verlag: Berlin, 1989; p 1.
11. Morgan, S. E.; McCormick, C. L. Prog Polym Sci 1990, 15, 507.
12. Shin, H. Ph.D. Thesis, Massachusetts Institute of Technology, 1965.
13. Lumley, J. L. Appl Mech Rev 1967, 20, 1139.
14. Schummer, P.; Thielen, W. Chem Eng Commun 1981, 4, 593.
15. Giesekus, H. Lecture Series. 1981–86; Von Karman Institute for Fluid Dynamics: Rhode-Saint-Genese, Belgium.
16. Bewersdorff, H.-W.; Berman, N. S. Rheol Acta 1988, 27, 130.
17. Interthal, W.; Haas, R. In Proceedings of Euromech, 1981; Vol. 143, p 157.
18. Elata, C.; Burger, J.; Michlin, J.; Takserman, U. Phys Fluid 1977, 20(10), S49.
19. James, D. F.; McLaren, D. R. J Fluid Mech 1975, 97, 655.
20. Naudascher, E.; Killen, J. M. Phys Fluids 1977, 20, 280.
21. Marshall, R. J.; Metzner, A. B. Ind Eng Chem Fundam 1967, 6, 393.
22. Hassager, O. J Chem Phys 1974, 60, 2111.
23. Zimm, B. H., Ed. F. Eirich. Academic: New York, 1960; Vol. 3.
24. Safieddine, A. M. Ph.D. Thesis, University of Southern Mississippi, 1990.
25. Mumick, P. S.; Welch, P. M.; Salazar, L. C.; McCormick, C. L. Macromolecules 1994, 27, 323.
26. McCormick, C. L.; Hester, R. D.; Morgan, S. E.; Safieddine, A. M. Macromolecules 1990, 23, 2124.
27. McCormick, C. L.; Hester, R. D.; Morgan, S. E.; Safieddine, A. M. Macromolecules 1990, 23, 2132.
28. Morgan, S. E. Ph.D. Thesis, University of Southern Mississippi, 1988; p 201.
29. Mumick, P. S. Ph.D. Thesis, University of Southern Mississippi, 1993; p 196.
30. Garner, C. M.; Springfield, R. M.; Cowan, M. E.; Hester, R. D. Stimuli-Responsive Water-Soluble and Amphiphilic (Co)polymers; McCormick, C. L., Ed.; ACS Symposium Series; American Chemical Society: Washington, DC, 2000.
31. Hoke, D.; Robins, R. J Polym Sci 1971, 10, 3311.
32. Blackmon, K. P. Ph.D. Thesis, University of Southern Mississippi, 1986.
33. Kathmann, E. E. L. Ph.D. Thesis, University of Southern Mississippi, 1994.
34. McCormick, C. L.; Hutchinson, B. H. Polymer 1988, 27, 623.
35. Huggins, M. L. J Am Chem Soc 1942, 64, 2716.
36. Kraemer, E. O. Ind Eng Chem 1938, 30, 1200.
37. McCormick, C. L.; Blackmon, K. P. Macromolecules 1986, 19, 1512.
38. Salazar, L. C. Ph.D. Thesis, University of Southern Mississippi, 1991.
39. Lumley, J. L. J Polym Sci Macromol Rev 1973, 7, 263.